Attitude Determination and Control System for the QuantSat-PT project (2022)

J. REVÉS
Instituto Superior Tecnico, Lisboa, Portugal

***Abstract*— The Attitude Determination and Control System (ADCS) of a satellite is the subsystem responsible for providing attitude knowledge and maintaining accurate pointing of the mission's payload. The objective of this work is to provide a functional ADCS to the QuantSat-PT project, a CubeSat developed to test the implementation of quantum communications. The mission requires high pointing accuracy, whilst being constrained by severe volume limits, as well as various manoeuvres besides Earth pointing. With this in mind, the payload's beacon detection is repurposed as a sensor, to provide an Earth's reference, in order to improve attitude estimation and comply with the combined pointing accuracy of $0.1°$. The beacon measurement is limited in its availability, so the sensors suite is complemented by a magnetometer, sun sensors and a gyroscope. Although reaction wheels are the most common actuator for high pointing accuracies, magnetorquers are used for further manoeuvres. A comparison between the multiplicative extended Kalman filter (MEKF), Complementary Filter (CF) and TRIAD algorithms is performed for the attitude determination. For the attitude control, a sliding controller, a global finite-time attitude tracking controller (GFTAC) and a simple proportional derivative (PD) controller are studied. The B-dot control law was employed for the detumbling manoeuvre. A simulation environment allowed for an accurate comparison of the different options. The proposed ADCS maintained a pointing error lower than $0.1°$ for 28.29% of the time the satellite was flying over the ground station (GS), with a direct line of sight (LOS).**

***Index Terms*— Cubesat, Kalman filter, nonlinear control, attitude determination, attitude control, QuantSat-PT**

I. INTRODUCTION

IN the information age, it is crucial to create and maintain secure communications. One way of improving our current security standards is to use Quantum Key Distribution (QKD) methods, which allows two parties to exchange encryption keys with absolute confidence that any eavesdropping by a third party will be detected. QKD is based on photonic communication links. Ground-based links typically rely on optical fibers, which have non-negligible losses, thus limiting transmission distances to a few hundreds of kilometres. As such, satellite-based QKD is a promising approach to establish a global quantum network. The development of a reliable and efficient space-to-ground link is an important first step, which has been demonstrated by the Micius satellite [4]. The QuantSat-PT project is the first step of a larger and longer-term vision of developing quantum communication satellites and ground stations in Portugal, making the country autonomous in such sovereignty technologies, and integrating Portugal into the future European Quantum Communication Infrastructure.

The attitude determination and control system (ADCS) is the subsystem responsible for pointing the satellite to a specific location. From the mission objectives, the attitude requirements are defined. In order to ensure Quantum communications, an attitude error in the range of tens of microradians must be obtained whilst in eclipse. Due to restrictions imposed by the payload size, the volume available for sensors and actuators is reduced, which often leads to an increase in the cost of the satellite, if no performance cutbacks are possible. With this in mind, the telescope from the payload will be used not only for communications but also to provide a ground reference, which replaces other sensors.

A staged attitude determination system is proposed. The pointing requirements increase when more accurate sensors and actuators can be employed. The first stage consists of using the common ADCS sensors to receive a signal from the beacon being transmitted by the ground station (GS). The attitude pointing requirements for this stage are defined by the accuracy needed so that the beacon can be perceived by the telescope, equivalent to being within its field of view (FOV), where the payload is pointed at the GS with an attitude error of $10°$. The second stage uses the Earth's reference from the beacon to improve the attitude estimation, with the goal of obtaining a pointing error of $0.1°$. This value is defined by the amplitude of actuation of the fast-steering mirrors, the third and final stage. These first two stages are treated as one when it comes to the control and estimation algorithms if a pointing, estimation or combined is lowered than $10°$ and are the ADCS's responsibility.

The ADCS is also tasked with two additional manoeuvres: the detumbling and the radio communications. The former must reduce the satellite's angular velocity after deployment in less than one orbit; the former must point the satellite to nadir for radio communications. The accuracy required for radio communications is much lower than quantum communication, so it is safe to say that if the mission's goal is met, the requirement is also compliant.

II. MATHEMATICAL MODELS

A. Quaternion kinematics and dynamics

The quaternion is used as the attitude representation since it is the lowest-dimensional parameterization that is

J. REVÉS is with Instituto Superior Tecnico, Lisboa, Portugal (email:joao.reves@tecnico.ulisboa.pt)

free from singularities [7]. The quaternion is defined as

$$\mathbf{q}(\mathbf{e},\vartheta) = \begin{bmatrix} \mathbf{e}\sin(\vartheta/2) \\ \cos(\vartheta/2) \end{bmatrix}, \tag{1}$$

where $\mathbf{e}$ is the rotation axis and ϑ is the rotation angle. A three-component representation can be computed from the combination of the Euler axis and angle, with $\boldsymbol{\vartheta} \equiv \vartheta\mathbf{e}$. The quaternion kinematics are given by

$$\dot{\mathbf{q}} = \frac{1}{2}\Omega(\boldsymbol{\omega})\mathbf{q}, \tag{2}$$

with

$$\Omega(\boldsymbol{\omega}) = \begin{bmatrix} [\boldsymbol{\omega}\times] & -\boldsymbol{\omega} \\ \boldsymbol{\omega} & 0 \end{bmatrix}. \tag{3}$$

To characterize the angular velocity changes, the dynamics of the satellite must be taken into account. The relation between the torques and the angular velocity $\boldsymbol{\omega}$ is described as

$$J\dot{\boldsymbol{\omega}} = -[\boldsymbol{\omega}\times]J\boldsymbol{\omega} + L. \tag{4}$$

B. Sensor and Actuators models

As previously mentioned, the payload will be adapted as a sensor. However, it is not sufficient by itself for correct attitude estimation. A gyroscope, a magnetometer and Sun sensors are added to the suite.

The angular velocity measurement $\hat{\boldsymbol{\omega}}$ from the gyroscope is considered to be corrupted by noise, η_{arw}, as well as a slow-varying bias, $\boldsymbol{\beta}_g$. As such, the gyroscope model is given as

$$\hat{\boldsymbol{\omega}} = \boldsymbol{\omega} + \boldsymbol{\beta}_g + \eta_{arw} \tag{5}$$

$$\dot{\boldsymbol{\beta}}_g = 0. \tag{6}$$

The sensor perturbation η_{arw} can be interpreted as an independent zero-mean Gaussian white-noise process. The gyroscope used is TDK InvenSense MPU-9250 and it is assumed that the alignments and scaling factors have been calculated through ground tests.

The magnetic field measurement is defined as the true magnetic field vectors $\mathbf{B}$, corrupted by a bias $\boldsymbol{\beta}_B$ and Gaussian white-noise η_B, such as

$$\hat{\mathbf{B}} = \mathbf{B} + \boldsymbol{\beta}_B + \eta_B \tag{7}$$

with

$$E[\boldsymbol{\eta}_{mag}\boldsymbol{\eta}_{mag}^T] = \sigma_{mag}^2 I_3. \tag{8}$$

The magnetometer used is the Honeywell HMC5983, which has standard deviation σ_{mag} specified as $200nT$.

The optical measurement for the GS laser beacon is given as

$$\hat{b}_b = A_{\eta_b} b_b = A(e_1,\phi_b)A(e_2,\theta_b)A(e_3,\xi_b)b_b, \tag{9}$$

where b_b is the normalized direction vector of the GS, in the body frame. The Euler angles used to generate the noise rotation matrix A_{η_b} can be characterized as Gaussian white-noise. This measurement model is based on Star Trackers, converted from quaternions to a rotation matrix [2].

Similarly to the Beacon, the Sun sensor measurements are given as

$$\hat{b}_s = A_{\eta_s} b_s = A(e_1,\phi_s)A(e_2,\theta_s)A(e_3,\xi_s)b_s, \tag{10}$$

where b_{sun} is the normalized sun vector, in the body frame. The Euler angles used to generate the noise rotation matrix $A_{\eta_{sun}}$ can be characterized as Gaussian white noise, with different variances for boresight and cross-boresight axis. The Sun sensor used is the Solar MEMS ISS-D25, one per face of the satellite.

Due to the high accuracy required by the mission, the actuators' choice is simplified. The control momentum gyro is not suitable for CubeSat applications so the reaction wheels are chosen. For the detumbling manoeuvre magnetorquers are used.

The torque generated through a reaction wheel can be modelled through a second-order system of a DC-motor coupled to a flywheel [3]. This approach requires knowledge of the reaction wheel's motor parameters, such as armature inductance and resistance, as well as the flywheels parameters. None of these specifications are available in COTS reaction wheels, so a model was assumed based on a first-order system for the motor, maximum torque values and physical parameters. The highest angular velocity possible, positive or negative, that corresponds to maximum stored momentum, serves as saturation for the output torque. Jitter and control speed disturbances are also added to the wheel's angular velocity.

The torque generated by a magnetorquer is given by [1]

$$L_{mtq} = \mathbf{m} \times \mathbf{B}, \tag{11}$$

where the $\mathbf{m}$ is the commanded magnetic dipole moment vector generated by the coils and $\mathbf{B}$ is the local geomagnetic field vector expressed in terms of the body-frame components.

III. ATTITUDE ESTIMATION

For the attitude estimation, the algorithms are divided in two approaches: static and recursive methods. The static algorithm implemented is TRIaxial Attitude Determination (TRIAD) and for the recursive algorithms the Multiplicative Extended Kalman Filter (MEKF) and the Complementary Filter (CF) are selected.

A. TRIAD

The TRIAD algorithm generates an attitude estimate from only two measurements and estimates in two different frames (denoted by $\mathbf{b}$ and $\mathbf{r}$).

$$A = [\mathbf{w}_1\mathbf{w}_2\mathbf{w}_3][\mathbf{v}_1\mathbf{v}_2\mathbf{v}_3]^T = \sum_{i=1}^{3} \mathbf{w}_i\mathbf{v}_i^T \tag{12a}$$

$$\mathbf{v}_1 = \mathbf{r}_1, \quad \mathbf{v}_2 = \mathbf{r}_\times \equiv \frac{\mathbf{r}_1 \times \mathbf{r}_2}{||\mathbf{r}_1 \times \mathbf{r}_2||}, \quad \mathbf{v}_3 = \mathbf{r}_1 \times \mathbf{r}_\times \tag{12b}$$

Initial condition	$\hat{\mathbf{q}}(t_0) = \hat{\mathbf{q}}_0$
	$\hat{\boldsymbol{\beta}}(t_0) = \hat{\boldsymbol{\beta}}_0$
	$P(t_0) = P_0$
Gain	$K_k = P_k^- H_k^T \left(\hat{\mathbf{x}}_k^-\right) \left[H_k \left(\hat{\mathbf{x}}_k^-\right) P_k^- H_k^T \left(\hat{\mathbf{x}}_k^-\right) + H_k\right]$
	$H_k \left(\hat{\mathbf{x}}_k^-\right) = \left[\begin{array}{cc} \left[\hat{\mathbf{b}}_1^- \times\right] & 0_{3\times3} \\ \left[\hat{\mathbf{b}}_2^- \times\right] & 0_{3\times3} \\ \vdots & \vdots \\ \left[\hat{\mathbf{b}}_N^- \times\right] & 0_{3\times3} \end{array}\right]\Bigg\|_{t_k}$
Update	$P_k^+ = \left[I - K_k H_k \left(\hat{\mathbf{x}}_k^-\right)\right] P_k^-$
	$\Delta\hat{\mathbf{x}}_k^+ = K_k \left[\mathbf{y}_k - \mathbf{h}_k \left(\hat{\mathbf{x}}_k^-\right)\right]$
	$\Delta\hat{\mathbf{x}}_k^+ \equiv \left[\begin{array}{cc} \hat{\boldsymbol{\vartheta}}_k^{+T} & \Delta\hat{\boldsymbol{\beta}}_k^{+T} \end{array}\right]^T$
	$\mathbf{h}_k \left(\hat{\mathbf{x}}_k^-\right) = \left[\begin{array}{c} A\left(\hat{\mathbf{q}}^-\right)\mathbf{r}_1 \\ A\left(\hat{\mathbf{q}}^-\right)\mathbf{r}_2 \\ \vdots \\ A\left(\hat{\mathbf{q}}^-\right)\mathbf{r}_N \end{array}\right]\Bigg\|_{t_k}$
	$\hat{\mathbf{q}}^* = \hat{\mathbf{q}}_k^- + \frac{1}{2}\Xi\left(\hat{\mathbf{q}}_k^-\right)\boldsymbol{\delta}\hat{\vartheta}_k^+$
	$\hat{\mathbf{q}}_k^+ = \mathbf{q}^* / \left\|\mathbf{q}^*\right\|$
	$\hat{\boldsymbol{\beta}}_k^+ = \hat{\boldsymbol{\beta}}_k^- + \Delta\hat{\boldsymbol{\beta}}_k^+$
Propagation	$\hat{\boldsymbol{\omega}}(t) = \boldsymbol{\omega}_g(t) - \hat{\boldsymbol{\beta}}(t)$
	$\dot{\hat{\mathbf{q}}}(t) = \frac{1}{2}\Xi(\hat{\mathbf{q}}(t))\hat{\boldsymbol{\omega}}(t)$
	$\dot{P}(t) = F(t)P(t) + P(t)F^T(t) + G(t)Q(t)G^T(t)$

TABLE I

MEKF for mission mode.

- adapted from [7]

$$\mathbf{w}_1 = \mathbf{b}_1, \quad \mathbf{w}_2 = \mathbf{b}_\times \equiv \frac{\mathbf{b}_1 \times \mathbf{b}_2}{||\mathbf{b}_1 \times \mathbf{b}_2||}, \quad \mathbf{w}_3 = \mathbf{b}_1 \times \mathbf{b}_\times \tag{12c}$$

$$\hat{A}_{TRIAD} = \mathbf{b}_1\mathbf{r}_1^T + (\mathbf{b}_1 \times \mathbf{b}_\times)(\mathbf{r}_1 \times \mathbf{r}_\times)^T + \mathbf{b}_\times\mathbf{r}_\times^T \tag{12d}$$

B. CF

The CF fuses the high-frequency angular velocity measurements from the gyroscope with the low-frequency measurements from the other sensors [5] [6].

$$\dot{\hat{\mathbf{q}}} = \Omega(\hat{\boldsymbol{\omega}}_\mathcal{B} - \boldsymbol{\beta} + k_p\boldsymbol{\gamma}) \otimes \hat{\mathbf{q}} \tag{13}$$

$$\dot{\hat{\boldsymbol{\beta}}}_g = -k_g\boldsymbol{\gamma} \tag{14}$$

$$\boldsymbol{\gamma} = \sum_{i=1}^{N} k_i[\mathbf{b}_i\times]A(\hat{\mathbf{q}})\mathbf{r}_i \tag{15}$$

C. MEKF

The multiplicative attribute of the filter is due to the error quaternion expression that follows

$$\mathbf{q} = \delta\mathbf{q}(\delta\boldsymbol{\vartheta}) \otimes \hat{\mathbf{q}}. \tag{16}$$

Since the attitude kinematics are non-linear, an EKF structure must be used, where the quaternion is not estimated but a "local" state vector, composed of a rotation vector and an estimation error for the bias

$$\Delta\mathbf{x} = \begin{bmatrix} \delta\boldsymbol{\vartheta} \\ \Delta\boldsymbol{\xi} \end{bmatrix}. \tag{17}$$

The MEKF equations are given in Table I

IV. ATTITUDE CONTROL

The attitude control algorithms are responsible for firstly reducing the satellite angular rate after deployment and then pointing the payload in the correct direction. The sliding controller, the global finite-time attitude tracking controller (GFTAC) and the PD controller are implemented for Earth pointing.

A. Sliding controller

A sliding mode controller, also referred to as variable structure control, varies its control law based on the position of the state trajectory. A sliding surface was defined as

$$\mathbf{s} = (\boldsymbol{\omega} - \boldsymbol{\omega}_d) + ksign(\delta q_4)\boldsymbol{\delta}\mathbf{q}_{1:3}, \tag{18}$$

that leads to the control law

$$L = \bar{J}\{\frac{k}{2}[|\delta q_4|(\boldsymbol{\omega}_d - \boldsymbol{\omega}) - sign(\delta q_4)\boldsymbol{\delta}\mathbf{q}_{1:3} \times (\boldsymbol{\omega} + \boldsymbol{\omega}_d)] + \dot{\boldsymbol{\omega}}_d - G\bar{\mathbf{s}}\} + [\boldsymbol{\omega}\times]\bar{J}\boldsymbol{\omega}, \tag{19}$$

with

$$\bar{s}_i = sat(s_i, \epsilon_i), i = 1, 2, 3 \tag{20}$$

and

$$sat(s_i, \epsilon_i) \equiv \begin{cases} 1 & \text{for } s_i > \epsilon_i \\ \frac{s_i}{\epsilon_i} & \text{for } |s_i| \leq \epsilon_i \\ -1 & \text{for } s_i < \epsilon_i \end{cases}. \tag{21}$$

B. GFTAC

The GFTAC controller calculates the necessary torque to maintain a trajectory with

$$L_d = \bar{\boldsymbol{\omega}}_d^X \bar{J}\bar{\boldsymbol{\omega}}_d + \bar{J}A(\boldsymbol{\delta}\mathbf{q})\dot{\boldsymbol{\omega}}_d \tag{22}$$

and uses it to define the control law, that leads to

$$L(\mathbf{x}_1) = L_d - k_1\kappa_1(h\boldsymbol{\delta}\mathbf{q}, 1 - \alpha_1) - k_2 sat_{\alpha_2}\boldsymbol{\delta}\boldsymbol{\omega}, \mathbf{x}_1 \in C_1 \tag{23}$$

$$\mathbf{x}_1^+ = G_1(\mathbf{x}_1) = (\boldsymbol{\delta}\mathbf{q}, \boldsymbol{\delta}\boldsymbol{\omega}, s\bar{g}n(\delta q_4)), \mathbf{x}_1 \in D_1 \tag{24}$$

C. PD controller - without feedforward

A considerable simplification to the tracking case could be done by assuming that the attitude variation is much smaller than the controller and system response and treating it as a fixed attitude. This leads to the control law

$$L = -k_p\text{sign}(\delta q_4)\boldsymbol{\delta}\mathbf{q}_{1:3} - k_d(1 \pm \boldsymbol{\delta}\mathbf{q}_{1:3}^T\boldsymbol{\delta}\mathbf{q}_{1:3})\boldsymbol{\omega}. \tag{25}$$

D. Detumbling

carrhe proposed B-dot controller generates a magnetic dipole based on the rate of change of the Earth's magnetic field measured such that [1]

$$\mathbf{m} = \frac{k}{||\mathbf{B}||}\boldsymbol{\omega} \times \mathbf{b}. \tag{26}$$

The proposed control law is

$$L = -k(I_3 - \mathbf{b}\mathbf{b}^T)\boldsymbol{\omega}. \tag{27}$$

V. TESTING

In order to compare the different algorithms and sensor/actuators suite, a simulation environment was developed in Matlab 2020b and Simulink. The position motion of the satellite, Earth, Sun and Moon are pre-calculated in order to reduce computation time. The position and velocity of the Earth and Moon were propagated through Runge-Kutta 4^th order integration and the Sun's position is calculated. The celestial bodies' positions are used to calculated and propagate the satellite's position with resort to Runge-Kutta 8^th order integration. The magnetic field true model used is 12^{th} degree WMM2020 model, provided by Matlab. The GS location is defined as having coordinates $38°N\ 150°W$. Aiming to use them in a simulation environment, the coordinates are converted to the Earth-centered inertial frame and propagated. The sensors and actuators follow the previously presented models, with the parameters extracted from the datasheets.

In the onboard use, the Earth's magnetic field is estimated through the 5^{th} degree WMM2020, self-developed. The Sun vector true model and estimation use the same algorithm since it is suitable for onboard use. The GS vector is calculated from the estimated position from the GPS and the known position of the GS. In order to determine the desired quaternion and angular velocity a rotation matrix was calculated by adding constraints to the Rodrigues's rotation formula.

A. Detumbling

In order to test the detumbling manoeuvres a simulation is started with a $10°/s$ angular rate, the expected tumbling rate after leaving the launcher. After 1.3474 orbits the angular rate crosses the detumbled threshold of $5°/s$ and, with the use of the controllers, is slowed down further. Although the satellite is slowed down to the required threshold, it does so in more than one orbit.

B. Beacon effectiveness verification

In order to verify if the estimation accuracy is improved with the use of the beacon, a comparison of the two cases (with and without the beacon) is done using the MEKF. It is assumed that when the beacon is in the LOS it is also within the FOV of the telescope. The results are presented in Table II.

The addition of the beacon decreases the attitude estimation error drastically, especially when it is only considered the period where the GS is in the LOS of the satellite and can be used to improve estimation. The bias estimation without the use of the beacon results in higher accuracy and a smoother conversion to the real value. It can be concluded that the beacon has a positive impact on the estimation and should be used in the attitude estimation. However, the availability is limited due to only being available in eclipse and in LOS.

Mean	With beacon	Without beacon
Attitude error (°)}	0.7974	1.1611
Attitude error in LOS (°)	0.4429	1.7852
Bias error ($°/s$)	2.6433×10^{-4}	2.6012×10^{-4}

TABLE II

Attitude and bias estimation performace with and without beacon.

C. Comparison of estimation methods

To compare the attitude estimation methods, scenario are simulated using the same initial values for quaternion and velocity. For the MEKF and CF, the initial quaternion estimate used illustrates $5.3°$ of initial error. The results of the simulation can be seen in Table III and in Fig. 1.

Although the CF has a high mean attitude estimation error, it mainly results from the eclipse phase. When only the magnetometer and gyroscope are available the attitude error increases drastically. Its accuracy is not high enough in the mission area since it doesn't reach a $0.1°$ accuracy consistently. The bias estimate is also far from the real value. The TRIAD method has a consistent estimate, that is only slightly improved with the addition of the beacon. Since it only uses 2 measurements, it doesn't provide an estimate in eclipse. As it is a deterministic method it doesn't need to converge, which is useful to provide an initial estimate for other methods considering it has a low computational demand. The MEKF demonstrates an acceptable accuracy when the beacon is used, although it is not throughout the full duration of the LOS. This is due to the fact that it has a convergence period when the beacon is available. In eclipse, the estimation is also deteriorated, but not as much as the CF. This results in a better bias estimation, that is used to correct the angular velocity measurements in the propagation phase. Tests were done with only the propagation step in eclipse, but it was found that the update with only one measurement was still beneficial for the attitude estimation.

Mean	MEKF	TRIAD	CF
Attitude error (°)	0.9429	0.6775	25.1388
Attitude error in LOS (°)	0.3780	0.5224	2.3361
Bias error ($°/s$)	2.7×10^{-4}	N/A	0.4529

TABLE III

Comparison of the attitude estimation methods.

D. Comparison of control methods

To test the different control algorithms, a scenario was simulated where there was a large initial error and a non-zero angular rate. This allowed for the controllers to be tested in how they converged to the desired frame. The controllers were tuned to so that they do not surpass the detumbling threshold for the angular rate whilst converging or following the desired frame.

The results are presented in Table IV. As expected, the PD controller has a high angular velocity and angular error and is incapable to react to the fast attitude variations whilst overflying the GS. The sliding controller has the

Mean	GFTAC	Sliding	PD
Attitude control error ($^\circ$)	0.2244	1.1888	3.0028
Angular velocity error ($^\circ/s$)	0.0689	0.0637	0.073

TABLE IV

Comparison of controllers.

longest convergence time but when the desired frame is reached it has a much better performance than the PD controller. Although the angular velocity error is comparable to the GFTAC controller, the angular error while overflying the GS is larger. The GFTAC controller achieves an angular error below 0.1° throughout the simulation, after convergence.

E. Mission mode control and estimation

For the mission, the MEKF is selected as the estimation algorithm. In this scenario, the beacon is only available if the GS is in the LOS of the satellite and if it is within the FOV of the telescope. Namely, if the pointing error rises above 10° the sensor is not available. The TRIAD algorithm is run once for the initialization of the filter, out of eclipse so that it can use both the magnetometer and sun sensors. When it comes to the controller, the GFTAC was chosen for its consistency in pointing accuracy and low angular velocity error. The quaternion estimate was used to calculate $\boldsymbol{\delta q}$ and the bias was used to correct the angular velocity measurements from the gyroscope.

Fig. 2 shows the pointing error of the complete system. The highest values for the pointing error are observed in eclipse and are improved whilst the beacon is LOS. It can be said that the estimation is predominantly responsible for the errors then. The initialization of the filter with the TRIAD method resulted in lower overall errors throughout the simulation. A pointing error lower than 0.1° was accomplished for 28.29% of the time in LOS.

REFERENCES

[1] Giulio Avanzini and Fabrizio Giulietti. Magnetic detumbling of a rigid spacecraft. *Journal of Guidance, Control, and Dynamics*, 35(4):1326–1334, 2012.

[2] Jonghee Bae, Youdan Kim, and Hee Seob Kim. Satellite Attitude Determination and Estimation using Two Star Trackers. In *2010 AIAA Guidance, Navigation, and Control Conference*. American Institute of Aeronautics and Astronautics.

[3] Valdemir Carrara and Hélio K Kuga. Torque and speed control loops of a reaction wheel. *11th International Conference on Vibration Problems*, page 11.

[4] Sheng-Kai Liao. Satellite-to-ground quantum key distribution. *Nature 2017*, 549(7670):43–47.

[5] R. Mahony, T. Hamel, and J.-M. Pflimlin. Complementary filter design on the special orthogonal group SO(3). In *Proceedings of the 44th IEEE Conference on Decision and Control*, pages 1477–1484. IEEE.

[6] Robert Mahony, Tarek Hamel, and Jean-Michel Pflimlin. Nonlinear Complementary Filters on the Special Orthogonal Group. *2008 IEEE Transactions on Automatic Control*, 53(5):1203–1218.

[7] F. Landis Markley and John L. Crassidis. *Fundamentals of Spacecraft Attitude Determination and Control, 2014*. Springer New York.

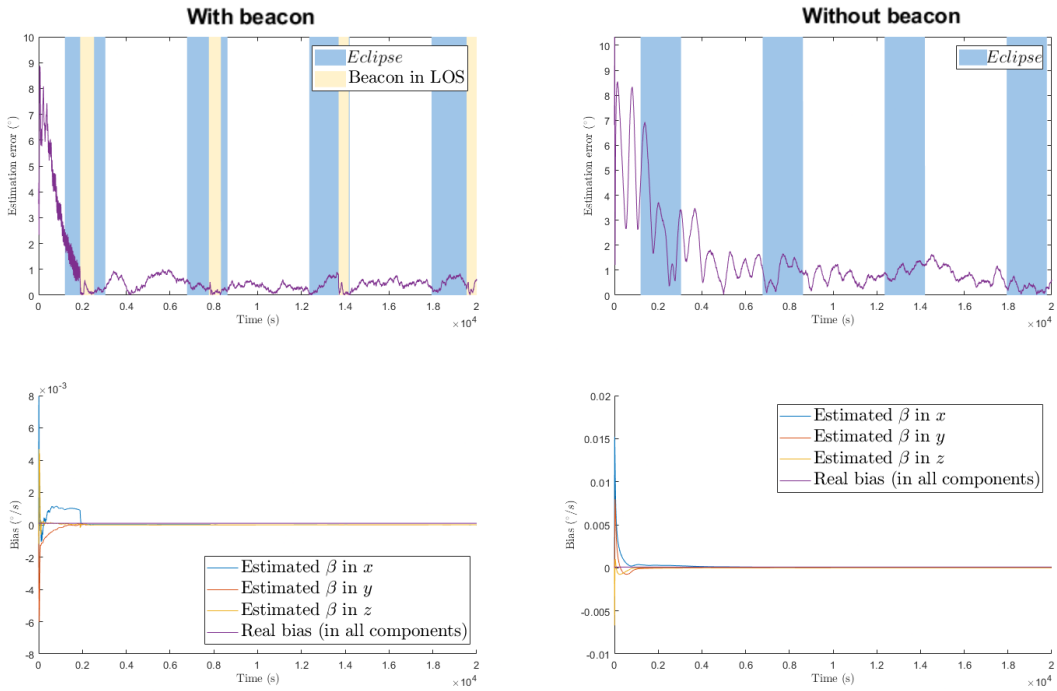

Fig. 1. Attitude (top) and bias (bottom) estimation with (left) and without (right) beacon.

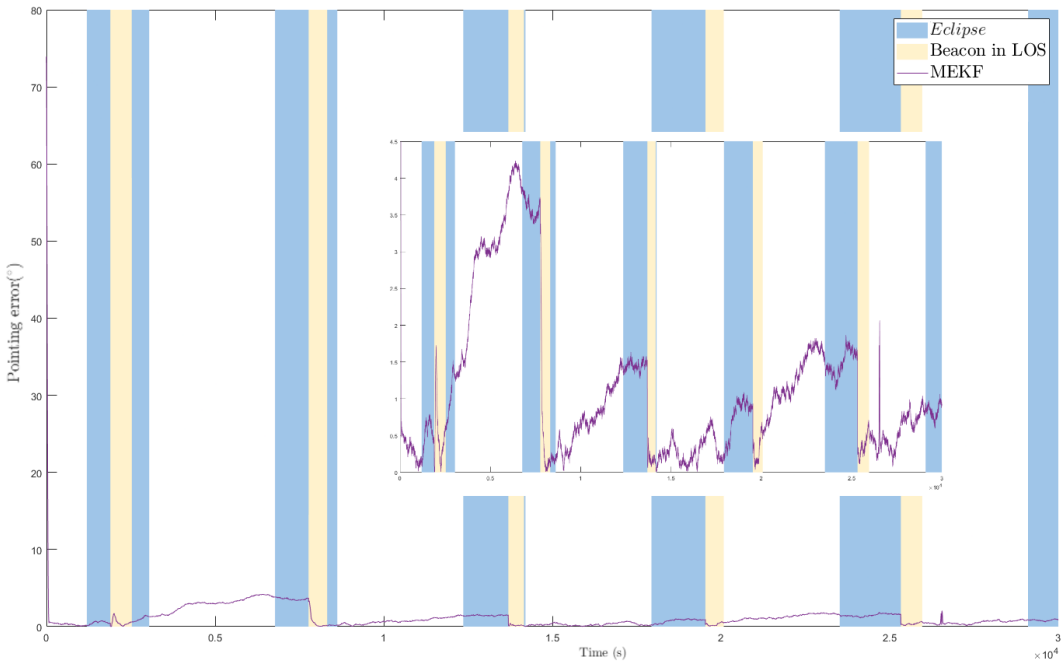

Fig. 2. Complete mission mode simulation with MEFK estimation and GFTAC control.